The Protoadamantane Radical Cation

Andrey A. Fokin,*[a] Boryslav A. Tkachenko,[a] Tatyana E. Shubina,[a] Pavel A. Gunchenko,[a] Dmitriy V. Gusev,[a] Jason K. Vohs,[b] Gregory H. Robinson,[b] Alexander G. Yurchenko,[a] and Peter R. Schreiner*[b,c]

Keywords: C-H activation / Density functional calculations / Electron transfer / Electrophilic additions / Radical ions

DFT (B3LYP) and MP2 computations with a 6-31G* basis set show that a unique protoadamantane radical cation ($\mathbf{1}^{\cdot+}$) structure with an elongated, half-broken C^6–H bond prevails both in the gas phase and in solution. This is in agreement with the observed regioselectivity of the single electron-transfer oxidation of protoadamantane (**1**) with photoexcited 1,2,4,5-tetracyanobenzene, which only gives 5-(6-protoadamantyl)-1,2,4-tricyanobenzene (**5**), for which the X-ray crystal structure is reported. The regioselectivities for the functionalizations of **1** with electrophiles support this oxidation pathway. The H-coupled electron-transfer mechanism recently proposed for the C–H activation of alkanes with electrophilic oxidizers explains the high C^6 positional selectivities in the functionalization of **1** in electrophilic media.

Introduction

Radical cations are key intermediates in alkane activations with strong oxidizers.[1,2] The removal of an electron from bonding molecular orbitals of saturated hydrocarbons gives so-called σ-radical cations:[3−9] a species characterized by partially broken σ_{C-C} and/or σ_{C-H} bonds.[10] Structural elucidations of such species are challenging both experimentally[4,6,8] and computationally,[11−21] due to facile rearrangements and the open-shell character of the respective wavefunctions. Even the qualitative results sensitively depend on the level of theory employed, especially for highly symmetrical hydrocarbons, which typically undergo Jahn−Teller distortions[22] (exceptions are known[23]) upon ionization. For instance, the methane radical cation[24] is a C_{2v}-symmetrical minimum at MP2 and QCISD, but it is a transition structure at several DFT levels.[25] Nevertheless, computations are an indispensable tool for investigations of these species; recent high-level ab initio and DFT computations on radical cations derived from simple alkanes[21,25,26] as well as from some cage hydrocarbons[18,27−34] typically agree well with photoelectron and low-temperature ESR spectra.[6,8,27,35−42]

Structural analyses of alkane radical cations are fundamental for a better understanding of the mechanisms of alkane functionalization with electrophiles when the activation occurs through polar (electron transfer, ET) transition structures. Our recent computational and experimental studies on the halogenation mechanisms of adamantane demonstrated that the 3° C−H regiospecificities can only be understood in terms of the adamantane moiety being largely radical cationic in the transition structures {the adamantane radical cation (C_{3v}) displays a half-broken 3° C−H bond}.[33] C−H activations with weakly electrophilic oxidants (such as Hal_n^+ or $Hal_{n-1}H^+$) are best visualized as concerted H-coupled electron transfer (HCET) involving linear $[R\cdots H\cdots E]^+$ fragments in the transition structures for hydrogen abstraction.

Protoadamantane (**1**) may challenge the HCET mechanistic concept because it, in contrast to adamantane, contains four different 3° C−H bonds with comparable dissociation energies; the protoadamantyl *tert*-carbocations are also comparably stable (vide infra). At the same time, C−H substitution in the protoadamantane cage (e.g., halogenation[43] and nitroxylation[44,45]) occurs regioselectively at the 6-position (Scheme 1), and such high selectivities cannot be explained in terms of purely electrophilic or radical mechanisms.

In this paper we present a computationally and experimentally based study of the oxidative transformations of protoadamantane. We emphasize the importance of the

[a] Department of Organic Chemistry, Kiev Polytechnic Institute
37 Pobeda Avenue, 03056 Kiev, Ukraine
Fax: (internat.) + 38-044/2742004
E-mail: aaf@xtf.ntu-kpi.kiev.ua
[b] Department of Chemistry, The University of Georgia,
Athens, Georgia 30602-2556, USA
Fax: (internat.) + 1-706/542-9454)
E-mail:prs@chem.uga.edu
[c] Institute of Organic Chemistry, Justus-Liebig-Universität Giessen,
Heinrich-Buff-Ring 58, 35392 Giessen, Germany
Fax: (internat.) + 49-(0)641/9934-309
E-mail: prs@org.chemie.uni-giessen.de
Supporting information for this article is available on the WWW under http://www.eurjoc.org or from the author.

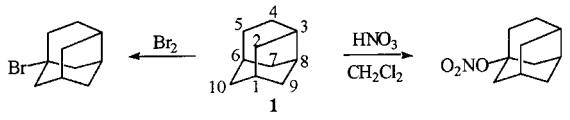

Scheme 1. The reactivity of protoadamantane (**1**) in the presence of electrophiles

newly developed HCET mechanistic model to ascertain the reactivity of protoadamantane in electrophilic media.

Results and Discussion

With a nondegenerate and delocalized HOMO (Figure 1), C_1 protoadamantane (**1**) is Jahn−Teller-inactive. Despite a number of possibilities for the formation of different ionized species with elongated 3° C−H bonds, all optimizations (BLYP, B3LYP, and MP2 with a 6-31G* basis set) of the protoadamantane radical cation ($\mathbf{1}^{\cdot+}$) give rise to a single structure with one elongated C^6−H bond (Figure 1). This finding can be explained by analysis of the HOMO coefficients (Figure 1), which are highest for $H^{6'}$ and C^6−C^8. Because of hyperconjugative interactions, the C^7−C^8 bond is elongated (1.6−1.7 Å in $\mathbf{1}^{\cdot+}$ vs. 1.53−1.55 Å in **1**) and the C^6−C^7 bond is shortened (to 1.51 Å). These bonds contribute most substantially to the charge/spin delocalization in $\mathbf{1}^{\cdot+}$.

To model the structure of $\mathbf{1}^{\cdot+}$ in solution, we computed a number of complexes of $\mathbf{1}^{\cdot+}$ with one and two explicit water molecules at the B3LYP/6-31G* level of theory. We located four 3° C−H complexes (**2a−d**, Figure 2 and Table 1) of $\mathbf{1}^{\cdot+}$ with one H_2O molecule: complex **2a** is the most stable. The geometry of the hydrocarbon part of **2a** is only slightly different from that of free $\mathbf{1}^{\cdot+}$: because of partial charge transfer to H_2O in **2a**, the C−C bonds in the protoadamantane cage are less different. The relative stabilities of complexes **2a−d** {$^{\cdot+}C^6$−H···OH_2 (**2a**, 0.0 kcal/mol) < $^{\cdot+}C^8$−H···OH_2 (**2b**, 1.6) < $^{\cdot+}C^3$−H···OH_2 (**2c**, 2.4) < $^{\cdot+}C^1$−H···OH_2 (**2d**, 3.2), B3LYP/6-31G* + ZPVE} are not entirely in agreement with those for the corresponding *tert*-protoadamantyl species (Table 1). The protoadamantyl C^6 cations and radicals are most favorable, while the C^1 cations and radicals are the least stable in this series; the C^3 species is more stable then C^8 {$^+C^6$ (0.0) < $^+C^3$ (3.3) < $^+C^8$ (5.9) < $^+C^1$ (7.4) and $^{\cdot}C^6$ (0.0) < $^{\cdot}C^3$ (0.8) < $^{\cdot}C^8$ (4.0) < $^{\cdot}C^1$ (5.0), B3LYP/6-31G* + ZPVE}. However, the relative stabilities for the C^3 and C^8 radical cation complexes interchange relative to those for cations and radicals (i.e., **2b** is more stable than **2c**). The relative instability of radical cation **2c** might be explained by unfavorable charge/density distributions, because the cage, with two elongated C^6−H and C^3−H bonds, is polarized in opposite directions.

We also computed some representative complexes of $\mathbf{1}^{\cdot+}$ with two water molecules (**3**), through the C^6−H/C^3−H (**3a**), C^6−H/C^1−H (**3b**), C^1−H/C^8−H (**3c**), and C^1−H/C^3−H (**3d**) bonds (Table 1) and we found the structures **3a** and **3b** to be most stable: **3a** (0.0) < **3b** (1.1) < **3c** (2.9) < **3d** (3.6) at B3LYP/6-31G* + ZPVE. Complexation with the water dimer does not affect the relative energy ordering, as the $^{\cdot+}C^6$−H···$(H_2O)_2$ (**4a**) complex is again more stable (2.0−2.5 kcal/mol) than $^{\cdot+}C^3$−H···$(H_2O)_2$ (**4b**) or $^{\cdot+}C^8$−H···$(H_2O)_2$ (**4c**). Hence, gas-phase and simple condensed-state computations imply that only one form of the protoadamantane radical cation ($\mathbf{1}^{\cdot+}$) − i.e., with an elongated, partially broken C^6−H bond − exists.

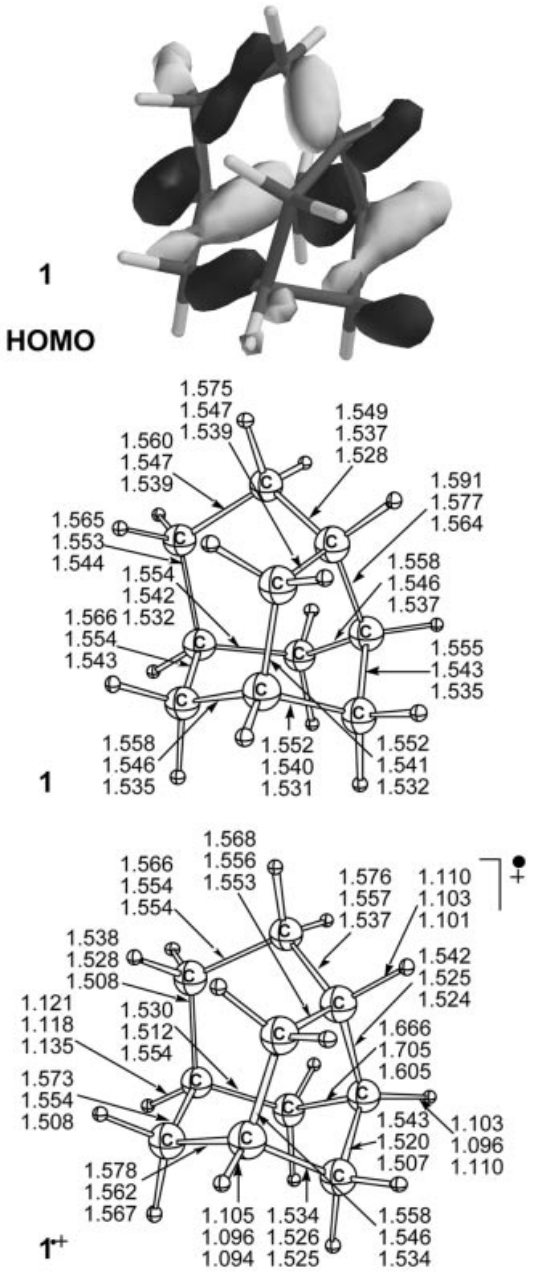

Figure 1. The HOMO of **1** and the BLYP- (first entries), B3LYP- (second entries), and MP2-optimized (third entries) geometries of protoadamantane (**1**) and the protoadamantane radical cation ($\mathbf{1}^{\cdot+}$) with a 6-31G* basis set (bond lengths in Å).

The most favorable transformation of $\mathbf{1}^{\cdot+}$ in the gas phase is hydrogen loss from the 6-position [Equation (1)].[34] In the condensed state, however, both proton [Equation (2)] and hydrogen losses [Equation (3)] giving 6-protoadamantyl

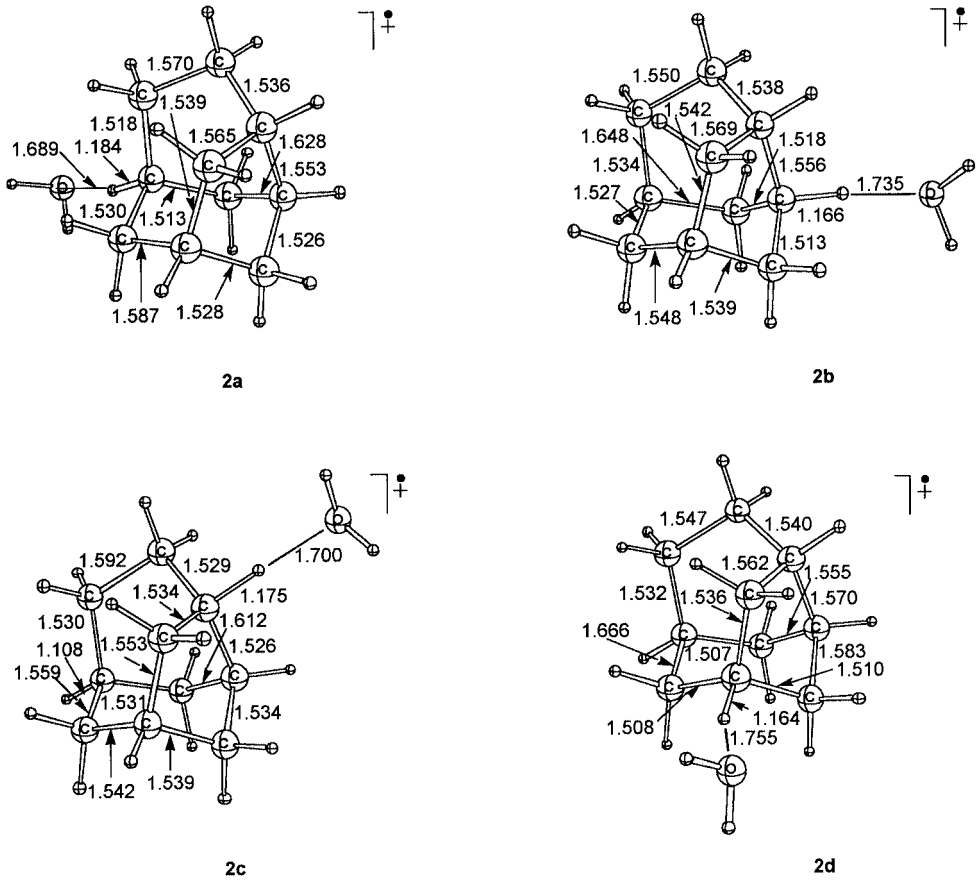

Figure 2. The B3LYP/6-31G*-optimized geometries of the complexes of the protoadamantane radical cation with water (bond lengths in Å)

Table 1. The energies for all computed species

Structure	B3LYP/6-31G* [−au]	ZPVE B3LYP/6-31G* [kcal/mol]
1	390.70785	153.3
1$^{\cdot+}$	390.37718	148.4
2a (C^6-H)	466.80737	163.9
2b (C^8-H)	466.80458	163.7
2c (C^3-H)	466.80278	163.4
2d (C^1-H)	466.80178	163.6
3a (C^3-H/C^6-H)	543.23084	178.5
3b (C^1-H/C^6-H)	543.22855	178.2
3c (C^1-H/C^8-H)	543.22511	177.8
3d (C^1-H/C^3-H)	543.22251	176.9
4a (C^6-H)	543.24739	180.3
4b (C^3-H)	543.24415	180.0
4c (C^8-H)	543.24387	180.3
6a (C^6-H)	3611.54329[a]	151.8[a]
6b (C^3-H)	3611.53974[a]	152.1[a]
6-ProtAd$^+$	389.81900	145.1
3-ProtAd$^+$	389.81337	144.9
8-ProtAd$^+$	389.80913	144.8
1-ProtAd$^+$	389.80699	145.0
6-ProtAd$^{\cdot}$	390.04363	144.7
3-ProtAd$^{\cdot}$	390.04214	144.6
8-ProtAd$^{\cdot}$	390.03751	144.9
1-ProtAd$^{\cdot}$	390.03648	144.9

[a] With the 6-31G** basis set.

species may take place. Hydrogen loss may even be more favorable (+19.0 for hydrogen vs. 32.3 kcal mol^{-1} for proton loss) because of the relatively high stability of the solvated 6-protoadamantyl cation [Equation (3)]. However, because of the higher solvation energy of H_3O^+ relative to 6-ProtAdHO_2^+, both reactions are close to thermoneutral if more than two explicit water molecules are included in the calculations.

$$\mathbf{1}^{\cdot+} \rightarrow \text{6-ProtAd}^+ + H^{\cdot} \quad +36.3 \text{ kcal/mol} \quad (1)$$

$$\mathbf{1}^{\cdot+} + H_2O \rightarrow \text{6-ProtAd}^{\cdot} + H_3O^+ \quad +32.3 \text{ kcal/mol} \quad (2)$$

$$\mathbf{1}^{\cdot+} + H_2O \rightarrow \text{6-ProtAdHO}_2^+ + H^{\cdot} \quad +19.0 \text{ kcal/mol} \quad (3)$$

In order to validate the behavior of **1**$^{\cdot+}$ in solution, we studied the oxidation of **1** in the presence of photoexcited 1,2,4,5-tetracyanobenzene (TCB), which is among the most powerful organic ET oxidants.[46,47] In complete agreement with the above computations, oxidation gives 5-(6-protoadamantyl)-1,2,4-tricyanobenzene (**5**) as the only product (Scheme 2), as a result of hydrogen loss from the C^6-H position of **1**$^{\cdot+}$. The X-ray structure of **5** is shown in Figure 3.

Thus, the oxidative ET functionalization of protoadamantane shows the same selectivity as electrophilic substitutions. We surmise that the structure of **1**$^{\cdot+}$ is the key for understanding the reactivity of **1** in electrophilic media. We

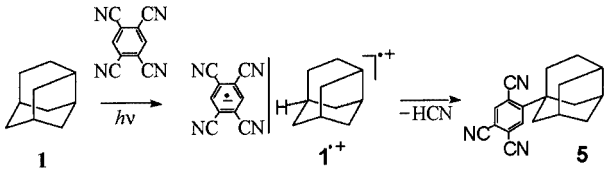

Scheme 2. The oxidation of protoadamantane (**1**) in the presence of photoexcited TCB

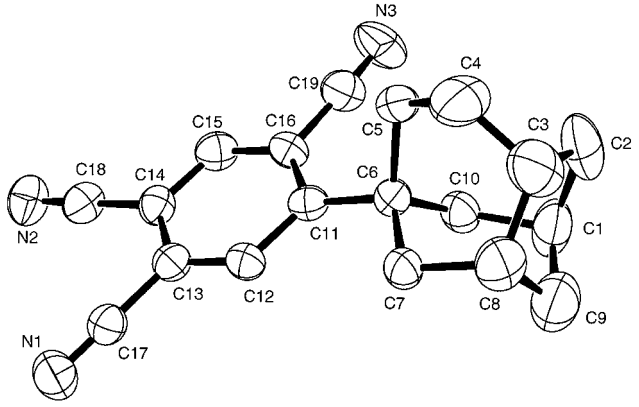

Figure 3. The X-ray structure of **5**; hydrogens omitted for clarity

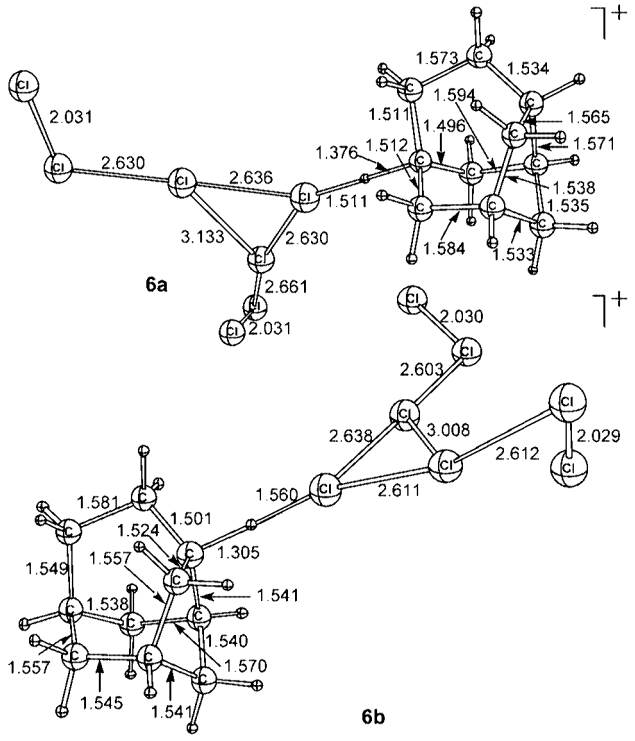

Figure 4. The B3LYP/6-31G**-optimized geometries of the transition structures for the reaction between **1** and Cl_7^+ (bond lengths in Å)

have previously modeled the reactions of adamantane with halogen electrophiles Hal_n^+ (n = 3, 5, and 7) for which the HCET transition structures describe the abstraction of a hydrogen from the tertiary position. Because of the system size (the Br_n^+ + protoadamantane reaction species are hard to compute at a proper level of theory), we used Cl_7^+ as a model electrophile. We found an analogous transition structure (**6a**, Figure 4) for **1** in reaction with Cl_7^+ describing the H-abstraction from the C^6-H position (the barrier is $\Delta G^{\ddagger}_{298}$ = 12.0 kcal/mol, B3LYP/6-31G**).

Structure **6a** is highly polarized (the total charge on the hydrocarbon moiety is +0.65 e); the geometry of the protoadamantane moiety in **6a** resembles the structure of the complex of **1**$^{\cdot+}$ with water (**2a**, vide supra). We also located the transition structure **6b** that describes the H-abstraction from the C^3-H position, but this reaction is 2.3 kcal/mol less favorable than that via **6a**. Other transition structures involving, for example, the C^8-H (**6c**) or C^1-H (**6d**) bonds are weakly bound clusters for rearrangements within the Cl_7^+ moiety rather than for H-abstraction. These findings are in agreement with the observed selectivity of the bromination of **1**,[43] in which 6-bromoprotoadamantane is formed. However, the existence of transition structure **6b** prompted us to reinvestigate the selectivity of this reaction. GC/MS analysis of the reaction mixture shows that, together with 6-bromoprotoadamantane, about 4% of 3-bromoprotoadamantane is formed; that is, the HCET reaction channel though the $[C^3\cdots H\cdots Hal_n]^+$ transition structure also exists.

The selectivities of the reactions of alkanes with electrophiles can be explained by analysis of the structures and stabilities of the respective radical cations. This was previously demonstrated for methane, isobutane, and adamantane.[48] The clear-cut reactivity of **1** with electrophiles is also in agreement with the HCET mechanism. Even for protoadamantane, which theoretically can give four different 3° $C-H$ substitution products, the singular nature of the radical cation **1**$^{\cdot+}$ translates into an exceedingly high C^6-H regioselectivity in electrophilic reactions.

Conclusions

The protoadamantane radical cation **1**$^{\cdot+}$ displays a structure with an elongated, electron-depleted C^6-H bond both in the gas phase and in solution. This is an agreement with the observed reactivity of protoadamantane **1** in the outer sphere electron-transfer oxidation with TCB, which gives only a single C^6-H substitution product. The electrophilic $C-H$ functionalization of **1** can be explained in terms of an inner sphere H-coupled electron-transfer (HCET) mechanism in which a distinct radical cationic hydrocarbon moiety in the transition structure is ultimately responsible for the regioselectivity.

Experimental Section

General Remarks: Geometries were fully optimized at the B3LYP/6-31G* (computed relative energies were ZPVE or ΔG corrected) and MP2/6-31G* levels of theory (unrestricted wavefunctions were used for open-shell species) as implemented in the Gaussian98 program package.[49] Harmonic vibrational frequencies were computed

to ascertain the nature of all stationary points (the number of the imaginary modes, NIMAG, is 0 for minima and 1 for transition structures). The geometries of the optimized species are collected in the Supporting Information.

NMR spectra were recorded with a Varian VXR-300 spectrometer at 300 MHz (^{1}H NMR) or 75 MHz (^{13}C NMR) in $CDCl_3$ solutions. The chemical shifts are given on the δ scale in ppm; internal standard HMDS. The GC/MS analyses were performed on an HP5890 with an H5971A detector (HP GC-MS capillary column 50 m-0.2 mm, Ultra1, Silicone, 80−250 °C, 10°/min).

Oxidation of Protoadamantane (1) with TCB: A solution of **1** (400 mg, 2.94 mmol) and TCB (315 mg, 1.76 mmol) in acetonitrile (400 mL) was irradiated under argon at 20 °C with a 450 W lamp (maximum emission at 350 nm) for 3 h. The NMR spectrum of the reaction mixture showed the signals of unchanged TCB and protoadamantane (**1**), as well as **5** as the only reaction product. The reaction mixture was diluted with water (40 mL) and the solvents (together with unchanged protoadamantane **1**) were removed in vacuo. Chromatographic separation on silica gel (*c*-C_6H_{12}/EtOAc, 7:3) gave TCB (160 mg, 0.89 mmol), together with 183 mg (0.64 mmol, 21.7%) of 5-(6-protoadamantyl)-1,2,4-tricyanobenzene (**5**, R_f = 0.55) as colorless crystals (m.p. 232−234 °C, acetonitrile). ^{1}H NMR: δ = 1.42 (m, 1 H), 1.72 (m, 7 H), 1.86 (m, 1 H), 2.12 (m, 1 H), 2.34 (s, 1 H), 2.47 (m, 3 H) 2.70 (m, 1 H), 7.80 (s, 1 H), 8.05 (s, 1 H) ppm. ^{13}C NMR: δ = 24.2, 32.7, 34.4, 35.6, 35.9, 36.0, 39.9, 40.9, 43.2, 113.5, 113.7, 114.5, 115.7, 117.0, 119.2, 131.0, 139.5, 162.0 ppm. IR ($CHCl_3$): $\tilde{\nu}$ = 2850−2290 (C−H), 2230 (C≡N), 1590−1650 (C=C) cm^{-1}. $C_{19}H_{17}N_3$: calcd. C 79.41; H 5.96; N 14.62.·; found C 79.25, H 6.16; N 14.43

Bromination of Protoadamantane (1): A mixture of protoadamantane (**1**, 0.15 g, 1.10 mmol) and bromine (1.41 g, 8.82 mmol) was kept at 23 °C for 16 h, poured onto an excess of a saturated solution of Na_2SO_3, and extracted with CH_2Cl_2 (3 × 10 mL), and the combined extracts were washed with water and dried with Na_2SO_4. Evaporation gave 220 mg of a mixture of **1**/6-bromoadamantane/3-bromoadamantane in a ratio of 0.30:1.00:0.05 according to GC/MS. 6-Protoadamantyl- and 3-protoadamantyl bromides were identified from standard samples prepared from 6-hydroxyprotoadamantane[50] and 3-hydroxyprotoadamantane,[51] respectively, by treatment with $SOBr_2$ in CCl_4.

X-ray Crystallographic Study: A colorless needle of **5**, $C_{19}H_{17}N_3$, approximately 0.80 mm × 0.30 mm × 0.20 mm, was used for the X-ray crystallographic analysis. The X-ray intensity data were measured at 293 K on a Siemens P4/SMART CCD-based X-ray diffractometer system equipped with a Mo-target X-ray tube (λ = 0.71073 Å) operated at 2000 W power. The detector was placed at a distance of 4.956 cm from the crystal.

A total of 1650 frames were collected with a scan width of 0.3° in ω or and an exposure time of 10 s/frame. The total data collection time was 7.80 h. The frames were integrated with the Bruker SAINT software package by use of a narrow-frame integration algorithm. The integration of the data using a triclinic unit cell yielded a total of 3774 reflections to a maximum 2θ angle of 46.52°, of which 2122 were independent with completeness = 98.4%, R_{int} = 2.67%. The final cell constants are *a* = 6.4536(19) Å, *b* = 7.671(2) Å, *c* = 15.542(5) Å, α = 90.223(5)°, β = 95.350(6)°, γ = 101.680(6)°, volume = 750.0(4) Å^3. Analysis of the data showed negligible decay during data collection. Data were corrected for absorption effects by the empirical method (SADABS) (ratio of minimum to maximum apparent transmission: 0.770).

The structure was solved and refined with the Bruker SHELXTL (Version 6.1) software package, using the group $P\bar{1}$ (No. 2), with Z = 2 for the formula unit $C_{19}H_{17}N_3$. The final anisotropic full-matrix, least-squares refinement on F^2 converged at $R1$ = 12.3%, $wR2$ = 30.1% and a goodness-of-fit of 1.058. The largest peak on the final difference map was 0.672 e$^-$/ Å^3. The calculated density for $C_{19}H_{17}N_3$ is 1.272 g/cm^3 and F(000) is 304 e$^-$. The non-hydrogen atoms were refined anisotropically, while hydrogen atoms were placed in ideal positions with their coordinates and thermal parameters riding on the attached carbon atoms.

CCDC 186319 contains the supplementary crystallographic data for this paper. These data can be obtained free of charge at www.ccdc.cam.ac.uk/conts/retrieving.html [or from the Cambridge Crystallographic Data Centre, 12, Union Road, Cambridge CB2 1EZ, UK; fax: (internat.) +44−1223/336-033; E-mail: deposit@ccdc.cam.ac.uk].

Acknowledgments

This work was supported by the Fundamental Research Foundation of the Ukraine, the Petroleum Research Fund (administrated by the American Chemical Society, P. R. S. and G. H. R.), and the NATO Science Program.

[1] A. A. Fokin, P. R. Schreiner, *Chem. Rev.* **2002**, *102*, 1551.
[2] A. Corma, *Chem. Rev.* **1995**, *95*, 559.
[3] H. D. Roth, H. X. Weng, D. H. Zhou, T. Herbertz, *Pure Appl. Chem.* **1997**, *69*, 809.
[4] S. McIlroy, H. X. Weng, H. D. Roth, *J. Phys. Org. Chem.* **1997**, *10*, 607.
[5] H. Weng, H. D. Roth, *J. Org. Chem.* **1995**, *60*, 4136.
[6] K. Ishiguro, I. V. Khudyakov, P. F. McGarry, N. J. Turro, H. D. Roth, *J. Am. Chem. Soc.* **1994**, *116*, 6933.
[7] C. J. Abelt, H. D. Roth, M. L. M. Schilling, *J. Am. Chem. Soc.* **1985**, *107*, 4148.
[8] L. B. Knight, Jr., G. M. King, J. T. Petty, M. Matsushita, T. Momose, T. Shida, *J. Chem. Phys.* **1995**, *103*, 3377.
[9] M. Schmittel, A. Burghart, *Angew. Chem. Int. Ed. Engl.* **1997**, *36*, 2551.
[10] D. J. Bellville, N. L. Bauld, *J. Am. Chem. Soc.* **1982**, *104*, 5700.
[11] G. J. Laming, N. C. Handy, R. D. Amos, *Mol. Phys.* **1993**, *80*, 1121.
[12] T. Clark, *Top. Curr. Chem.* **1996**, *177*, 1.
[13] C. W. Murray, N. C. Handy, *J. Chem. Phys.* **1992**, *97*, 6509.
[14] N. L. Ma, B. J. Smith, J. A. Pople, L. Radom, *J. Am. Chem. Soc.* **1991**, *113*, 7903.
[15] R. H. Nobes, D. Moncrieff, M. W. Wong, L. Radom, P. M. W. Gill, J. A. Pople, *Chem. Phys. Lett.* **1991**, *182*, 216.
[16] T. Bally, S. Bernhard, S. Matzinger, L. Truttmann, Z. D. Zhu, J.-L. Roulin, A. Marcinek, J. Gebicki, F. Williams, G.-F. Chen, H. D. Roth, T. Herbertz, *Chem. Eur. J.* **2000**, *6*, 849.
[17] T. Bally, L. Truttmann, S. Dai, F. Williams, *J. Am. Chem. Soc.* **1995**, *117*, 7916.
[18] G. N. Sastry, T. Bally, V. Hrouda, P. Cársky, *J. Am. Chem. Soc.* **1998**, *120*, 9323.
[19] J. H. Wang, A. D. Becke, V. H. Smith, *J. Chem. Phys.* **1995**, *102*, 3477.
[20] M. Sodupe, J. Bertran, L. Rodriguez-Santiago, E. J. Baerends, *J. Phys. Chem. A* **1999**, *103*, 166.
[21] H. M. Sulzbach, D. Graham, J. C. Stephens, H. F. Schaefer, *Acta Chem. Scand.* **1997**, *51*, 547.
[22] I. B. Bersuker, *Chem. Rev.* **2001**, *101*, 1067.
[23] A. A. Fokin, P. R. Schreiner, P. v. R. Schleyer, P. A. Gunchenko, *J. Org. Chem.* **1998**, *62*, 6494.
[24] R. J. Boyd, K. V. Darvesh, P. D. Fricker, *J. Chem. Phys.* **1991**, *94*, 8083.

[25] S. D. Wetmore, R. J. Boyd, L. A. Eriksson, A. Laaksonen, *J. Chem. Phys.* **1999**, *110*, 12059.
[26] H. Zuilhof, J. P. Dinnocenzo, A. C. Reddy, S. Shaik, *J. Phys. Chem.* **1996**, *100*, 15774.
[27] A. D. Trifunac, D. W. Werst, R. Herges, H. Neumann, H. Prinzbach, M. Etzkorn, *J. Am. Chem. Soc.* **1996**, *118*, 9444.
[28] T. Clark, *Acta Chem. Scand.* **1997**, *51*, 646.
[29] Y. Inadomi, K. Morihashi, O. Kikuchi, *J. Mol. Struct. (Theochem)* **1998**, *434*, 59.
[30] Y.-J. Liu, M.-B. Huang, *J. Mol. Struct. (Theochem)* **2001**, *536*, 133.
[31] O. Wiest, *J. Phys. Chem.* **1999**, *103*, 7907.
[32] P. R. Schreiner, A. Wittkopp, P. A. Gunchenko, A. I. Yaroshinsky, S. A. Peleshanko, A. A. Fokin, *Chem. Eur. J.* **2001**, *7*, 2739.
[33] A. A. Fokin, P. A. Gunchenko, S. A. Peleshanko, P. v. R. Schleyer, P. R. Schreiner, *Eur. J. Org. Chem.* **1999**, 855.
[34] A. A. Fokin, P. R. Schreiner, P. A. Gunchenko, S. A. Peleshanko, T. E. Shubina, S. D. Isaev, P. V. Tarasenko, N. I. Kulik, H.-M. Schiebel, A. G. Yurchenko, *J. Am. Chem. Soc.* **2000**, *122*, 7317.
[35] K. Toriyama, K. Nunome, M. Iwasaki, *J. Chem. Phys.* **1982**, *77*, 5891.
[36] K. Takeshita, *J. Chem. Phys.* **1987**, *86*, 329.
[37] K. Toriyama, *Chem. Phys. Lett.* **1991**, *177*, 39.
[38] K. Toriyama, M. Okazaki, K. Nunome, K. Matsuura, *Radiat. Phys. Chem.* **1991**, *37*, 15.
[39] M. Iwasaki, K. Toriyama, K. Nunome, *J. Chem. Soc., Chem. Commun.* **1983**, 202.
[40] K. Ushida, T. Shida, M. Iwasaki, K. Toriyama, K. Nunome, *J. Am. Chem. Soc.* **1983**, *105*, 5496.
[41] F. Gerson, X.-Z. Qin, C. Ess, E. Kloster-Jensen, *J. Am. Chem. Soc.* **1989**, *111*, 6456.
[42] X.-Z. Qin, A. D. Trifunac, P. E. Eaton, Y. Xiong, *J. Am. Chem. Soc.* **1991**, *113*, 669.
[43] A. Karim, M. A. McKervey, *J. Chem. Soc., Perkin Trans. 1* **1974**, 2475.
[44] Y. N. Klimochkin, O. V. Abramov, I. I. Moiseev, M. F. Vologin, M. V. Leonova, E. I. Bagrii, *Petr. Chem.* **2000**, *40*, 415.
[45] Y. N. Klimochkin, E. O. Zhilkina, O. V. Abramov, I. I. Moiseev, *Zhurn. Org. Khim.* **1993**, *29*, 1358.
[46] M. Mella, M. Freccero, T. Soldi, E. Fasani, A. Albini, *J. Org. Chem.* **1996**, *61*, 1413.
[47] M. Mella, M. Freccero, A. Albini, *Tetrahedron* **1996**, *52*, 5533.
[48] A. A. Fokin, T. E. Shubina, P. A. Gunchenko, S. D. Isaev, A. G. Yurchenko, P. R. Schreiner, *J. Am. Chem. Soc.* **2002**, *124*, 10718.
[49] M. J. Frisch, G. W. Trucks, H. B. Schlegel, G. E. Scuseria, M. A. Robb, J. R. Cheeseman, V. G. Zakrzewski, J. A. J. Montgomery, R. E. Stratmann, J. C. Burant, S. Dapprich, J. M. Millam, A. D. Daniels, K. N. Kudin, M. C. Strain, O. Farkas, J. Tomasi, V. Barone, M. Cossi, R. Cammi, B. Mennucci, C. Pomelli, C. Adamo, S. Clifford, J. Ochterski, G. A. Petersson, P. Y. Ayala, Q. Cui, K. Morokuma, D. K. Malick, A. D. Rabuck, K. Raghavachari, J. B. Foresman, J. Cioslowski, J. V. Ortiz, B. B. Stefanov, G. Liu, A. Liashenko, P. Piskorz, I. Komaromi, R. Gomperts, R. L. Martin, D. J. Fox, T. Keith, M. A. Al-Laham, C. Y. Peng, A. Nanayakkara, C. Gonzalez, M. Challacombe, P. M. W. Gill, B. Johnson, W. Chen, M. W. Wong, J. L. Andres, M. Head-Gordon, E. S. Replogle, J. A. Pople, *Gaussian98*, Rev. A. 9, Pittsburgh PA, **1998**.
[50] J. Janjatovic, Z. Majerski, *J. Org. Chem.* **1980**, *45*, 4892.
[51] E. L. Tae, C. Ventre, Z. D. Zhu, I. Likhotvorik, F. Ford, E. Tippmann, M. S. Platz, *J. Phys. Chem.* **2001**, *105*, 10146.

Received May 28, 2002
[O02289]